Wittmann, H., von Blanckenburg, F., Mohtadi, M., Christl, M., Bernhardt, A. (2017): The competition between coastal trace metal fluxes and oceanic mixing from the 10Be/9Be ratio: Implications for sedimentary records. - *Geophysical Research Letters*, *44*, 16, pp. 8443—8452.

DOI: http://doi.org/10.1002/2017GL074259

AGU PUBLICATIONS

Geophysical Research Letters

RESEARCH LETTER
10.1002/2017GL074259

Key Points:
- Meteoric $^{10}Be/^{9}Be$ in marine sediments shows terrestrial signals overprinted by seawater ratios 30 km offshore Chile coast (37°S)
- Net loss of reactive Fe and Be metals from pore water to sedimentary phase provides evidence for boundary exchange mechanism
- Implications for $^{10}Be/^{9}Be$ in marine records for paleodenudation flux reconstructions are that exchange with seawater cannot be neglected

Supporting Information:
- Supporting Information S1

Correspondence to:
H. Wittmann,
wittmann@gfz-potsdam.de

Citation:
Wittmann, H., F. von Blanckenburg, M. Mohtadi, M. Christl, and A. Bernhardt (2017), The competition between coastal trace metal fluxes and oceanic mixing from the $^{10}Be/^{9}Be$ ratio: Implications for sedimentary records, *Geophys. Res. Lett.*, *44*, 8443–8452, doi:10.1002/2017GL074259.

Received 22 MAY 2017
Accepted 28 JUL 2017
Accepted article online 31 JUL 2017
Published online 19 AUG 2017

The competition between coastal trace metal fluxes and oceanic mixing from the $^{10}Be/^{9}Be$ ratio: Implications for sedimentary records

H. Wittmann[1], F. von Blanckenburg[1,2], M. Mohtadi[3], M. Christl[4], and A. Bernhardt[2]

[1]GFZ German Research Centre for Geosciences, Section 3.3 Earth Surface Geochemistry, Potsdam, Germany, [2]Department of Geosciences, Freie Universität Berlin, Berlin, Germany, [3]MARUM-Center for Marine Environmental Sciences, University of Bremen, Bremen, Germany, [4]Laboratory of Ion Beam Physics, Department of Physics, ETH Zurich, Zurich, Switzerland

Abstract At an ocean margin site 37°S offshore Chile, we use the meteoric cosmogenic $^{10}Be/^{9}Be$ ratio to trace changes in terrestrial particulate composition due to exchange with seawater. We analyzed the marine authigenic phase in surface sediments along a coast-perpendicular transect and compared to samples from their riverine source. We find evidence for growth of authigenic rims through coprecipitation, not via reversible adsorption, that incorporate an open ocean $^{10}Be/^{9}Be$ signature from a deep water source only 30 km from the coast, overprinting terrestrial $^{10}Be/^{9}Be$ signatures. Together with increasing $^{10}Be/^{9}Be$ ratios, particulate-bound Fe concentrations increase, which we attribute to release of Fe-rich pore waters during boundary exchange in the sediment. The implications for the use of $^{10}Be/^{9}Be$ in sedimentary records for paleodenudation flux reconstructions are the following: in coast-proximal sites the authigenic record will likely preserve local riverine ratios unaffected by exchange with seawater, whereas sites beneath well-mixed seawater will preserve global flux signatures.

1. Introduction

Marine sediments provide continuous archives of the sedimentary trace metal flux from the continents to the world's oceans. Among the many elemental and isotope ratio proxies in use to infer trace metal fluxes [*Jeandel and Oelkers*, 2015], the much overlooked ratio of the meteoric cosmogenic nuclide ^{10}Be to the stable ^{9}Be offers particular advantages: the seawater $^{10}Be/^{9}Be$ ratio combines a nuclide produced in the atmosphere at a relatively known rate with a stable isotope that records the unknown continental weathering and erosion flux. In seawater the $^{10}Be/^{9}Be$ ratio thus provides important information on, e.g., mixing of reactive trace metals. When measured on the authigenic phase of marine sediments, the $^{10}Be/^{9}Be$ ratio allows deriving the feedbacks between erosion, weathering, and climate in the geologic past [e.g., *Willenbring and von Blanckenburg*, 2010a; *von Blanckenburg et al*., 2015]. The $^{10}Be/^{9}Be$ ratio in authigenic phases is also used to constrain chronologies of marine sediments, of ^{10}Be deposition rates, and variations of Earth's magnetic field [e.g., *Kusakabe and Ku*, 1984; *Segl et al*., 1984; *Bourlès et al*., 1989a; *Christl et al*., 2003; *Carcaillet et al*., 2004; *Knudsen et al*., 2008; *Ménabréaz et al*., 2014; *Simon et al*., 2016a, 2017].

Essential to this present study is the new framework by *von Blanckenburg and Bouchez* [2014], which establishes the $^{10}Be/^{9}Be$ as a proxy of continental weathering and denudation that can be applied to marine archives. When ^{9}Be is released from bedrock during weathering and introduced to the ocean in the dissolved form, is it mixed with dissolved meteoric ^{10}Be, which is mainly delivered to the ocean through direct atmospheric deposition. As Be is particle reactive, formerly dissolved $^{10}Be/^{9}Be$ is preserved in marine authigenic phases as amorphous coating on sediment or is incorporated into Fe-Mn crusts. The main underlying assumption to the framework of *von Blanckenburg and Bouchez* [2014] is that dissolved Be isotopes are well mixed before being incorporated into marine authigenic phases. Despite the inherently different sources of both isotopes, homogenization by ocean gyres proceeds efficiently, with only low dispersion of dissolved $^{10}Be/^{9}Be$ [*von Blanckenburg and Igel*, 1999]. The sensitivity of the $^{10}Be/^{9}Be$ as a paleoproxy of continental denudation arises from the short residence time of Be in the ocean (0.2–1 kyr) [*Kusakabe et al*., 1990; *Lao et al*., 1992; *von Blanckenburg et al*., 1996] being shorter than ocean water mixing times. The short residence time is largely resulting from high scavenging intensities at ocean margins [*Anderson et al*., 1990]. When reaching the ocean floor, formerly scavenged Be might be partly released again into pore waters [*Bourlès et al*., 1989b] by so-called boundary exchange during early diagenetic reductive processes coupled to the iron redox cycle

[*Lacan and Jeandel*, 2005; *Arsouze et al*., 2009; *Radic et al*., 2011; *Wilson et al*., 2012]. This release of Fe, Be, and other metals from sediments to pore waters during boundary exchange may provide an important transfer mechanism between sediment and seawater [e.g., *Anderson et al*., 2014; *Jeandel and Oelkers*, 2015]. Given the power of meteoric ^{10}Be and the ^{10}Be/^{9}Be ratio in seawater and sediment to reconstruct processes like riverine and dust metal inputs [*Brown et al*., 1992a; *von Blanckenburg et al*., 1996; *Frank et al*., 2009], estuarine removal [*Kusakabe et al*., 1991], boundary scavenging [*Anderson et al*., 1990], trace metal mixing [*Igel and von Blanckenburg*, 1999; *von Blanckenburg and Igel*, 1999], and pore water mobility of metals [*Bourlès et al*., 1989b], it is surprising that this system did not find mentioning in recent reviews of elemental and isotope proxies for marine trace metal cycles [*Jeandel and Oelkers*, 2015; *Jeandel*, 2016].

In particular, regarding the boundary exchange process, the ^{10}Be/^{9}Be allows to evaluate the sites, the mass fluxes, and hence the efficiency of this process. Locating the sites of exchange in turn is required to identify the oceanic environment in which authigenic ^{10}Be/^{9}Be ratios can be used to faithfully reconstruct continental weathering [*von Blanckenburg and Bouchez*, 2014] or the cosmic ray variations resulting from changes Earth's magnetic field strength [*Simon et al*., 2016a].

In a continental margin setting at ~37°S offshore Chile we investigated the change in the particulate-bound terrestrial ^{10}Be/^{9}Be due to exchange with seawater. We sampled marine surface sediments covering lateral distances of 30 to 80 km from the coast along a coast-perpendicular transect. The transect, together with samples from river basins comprising the main sediment source to the shelf, allowed to investigate the change in the ^{10}Be/^{9}Be ratio from the terrestrial source to the oceanic sink.

2. Study Site, Sampling, and Origin of Terrigenous Sediments

At the Pacific coast between 37° and 38°S, sediment input into the ocean is mainly fluvial, as opposed to predominate aeolian input in northern Chile [*Lamy et al*., 1998]. We therefore sampled detrital sediment from the Biobío, Lebu, and Yani Rivers (termed Terra 1–3; Table 1 and Figure 1) close to their coastal outlets, and marine surface sediment offshore central Chile from four multicorer (MUC) cores obtained during *RV Sonne* cruise SO-156 [*Hebbeln and Cruise Participants*, 2001]. The four MUC sites together comprise a coast-perpendicular transect located at 37.4°S (Figure 1), from site MUC-1 located just off the shelf edge at approximately 30 km from the Chilean coast to site MUC-4 located at a distance of 80 km from the coast. MUC-4 is located within the northward inclined subduction trench, whereas MUC sites 1–3 sites are located on the steep continental slope. Surface ocean currents prevailing at our sampling sites (Figure 1) comprise the northward directed coastal Peru-Chile Current extending to ~100 km offshore. Beneath this current in ~200–300 m water depth, the southward directed Gunther Undercurrent flows mainly over the outer shelf and the continental slope [*Strub et al*., 1998]. The Gunther Undercurrent is presumably moving material southward before it sweeps sediment onto the continental slope and is also inferred to transport sediment from the Biobío River outlet to the more southern MUC sites [*Bernhardt et al*., 2016]. Thus, the coastal Terra catchments comprise the main sediment source to the adjacent continental shelf probed by MUC samples, as along the steep slope segment, downslope sediment transport dominates, and the surface sediment and Holocene turbidites generally mirror the upland provenance [*Lamy et al*., 1998; *Heberer et al*., 2010].

3. Methods

Authigenic phases such as amorphous Fe-Al oxyhydroxides and reactive Fe-Mn surfaces are the main carrier of meteoric ^{10}Be in the ocean [*Bourlès et al*., 1989a]. These so-called "reactive" phases can be obtained from sequential extractions. We performed the extraction method of *Wittmann et al*. [2012] that is based on a protocol developed for marine sediments [*Tessier et al*., 1979; *Bourlès et al*., 1989a; *Brown et al*., 1992b]. All resulting concentrations of reactive Be (termed $[^{9}Be]_{reac}$ and $[^{10}Be]_{reac}$) and those of major elements are calculated relative to the initial solid sample mass prior to extraction.

The sequential extraction steps were performed on several grain size fractions (Table 1), depending on sample recovery. Laser granulometry (Table S5) revealed that sieved grain size fractions are only apparent, as also much smaller particles were found that formed larger aggregated grains.

Extracted solutions were digested and purified for cosmogenic ^{10}Be measurements according to established methods (see supporting information). Using accelerator mass spectrometry measurements [*Christl et al*.,

Geophysical Research Letters

10.1002/2017GL074259

Table 1. Sample Characteristics and Mineralogical Composition of Terrestrial and Marine Sediments[a]

Sample ID	River or Core Label[b]	Latitude (°S)	Longitude (°W)	Terrestrial Drainage Area (km^2)	Sediment Load From In Situ ^{10}Be[c] (Mt/yr)	Water Depth (m)	Distance From Coast (km)	Mineralogical Composition From XRD Analysis (in wt %) of Silicate Residuum								
								Grain Size Analyzed[d] (μm)	Quartz	Plagioclase	Amphibole	Kaolinite	Muscovite and Illite	Chlorite	Amorphous[e]	Clinoptilolite
Terra-1[g]	Bíobío	36.81	73.17	6440[f]	0.75	-	0	<63	8.3	56.9	7.8	13.3	11.0	n.d.	n.d.	n.d.
Terra-2	Lebu	37.54	73.38	798	0.052	-	0	<63	20.6	23.6	n.d.	23.6	30.5	n.d.	n.d.	1.7
Terra-3	Yani	37.42	73.53	114	0.047	-	0	<63	21.0	39.7	n.d.	12.2	27.1	n.d.	n.d.	n.d.
Terra: XRD data weighed for sediment load measured by in situ ^{10}Be[h]									9.8	53.9	-	13.9	13.1	-	-	-
MUC-1[i]	GeoB7171	37.40	73.95	-	-	−1386	30	<63	8.9	38.7	<1.6	27.9	13.9	<1.7	5.1	n.d.
Replicate of MUC-1		37.40	73.95	-	-	−1386	30	125–250	7.4	48.5	d.l.	25.9	11.4	n.d.	6.8	n.d.
MUC-2	GeoB7170	37.40	74.14	-	-	−2229	42	63–125	10.2	62.6	1.4	6.2	19.3	n.d.	d.l.	0.4
MUC-3	GeoB7169	37.40	74.32	-	-	−3249	62	125–250	10.9	54.8	n.d.	6.8	27.6	n.d.	d.l.	n.d.
MUC-4	GeoB7168	37.40	74.51	-	-	−4650	80	63–125	10.2	46.7	n.d.	9.5	30.8	2.9	d.l.	n.d.

[a] n.d. = not determined; d.l. = close to detection limit.

[b] "GeoB" obtained during cruise SO-156 (*RV Sonne*) in 2001 [*Hebbeln and Cruise Participants*, 2001]. Sediment from the upper 0–1 cm layer was sampled. Due to very high modern sedimentation rates along this latitude (0.15–0.30 cm/yr) [*Muñoz et al.*, 2004], this layer should represent modern surface sediment.

[c] Sediment load derived from in situ cosmogenic ^{10}Be measured in river sand, calculated for "floodplain corrected" drainage area (comprising the sediments' source area) [see *Wittmann and von Blanckenburg*, 2016] and using the in situ ^{10}Be production scaling model of *Dunai* [2000] and a sea level high-latitude production rate of 3.75 at/g/yr [*Braucher et al.*, 2011; *Borchers et al.*, 2016]. Note that the in situ denudation rate of the Biobio River was obtained by *Tolorza-Tolorza* [2015]. We used these values to calculate "load-weighed" XRD and Be results (Table 2).

[d] Grain size obtained from dry sieving. These are apparent grain sizes due to secondary particle formation revealed by laser granulometry data evaluated according to *Blott and Pye* [2001] (see supporting information).

[e] Comprises a minimum as composition was determined on silicate residual (after sequential chemical leaching).

[f] Total drainage area at conception is 24,200 km^2; the value given is the "floodplain-corrected" high-relief area of the basin where sediment is being produced.

[g] This sample also contains 1.01 wt % of montmorillonite.

[h] Load-weighed values (for terrestrial samples) calculated by weighing each value with the respective in situ ^{10}Be-derived sediment load (see supporting information for methodology).

[i] This samples' grain size also contains <2.2 wt % of heulandite.

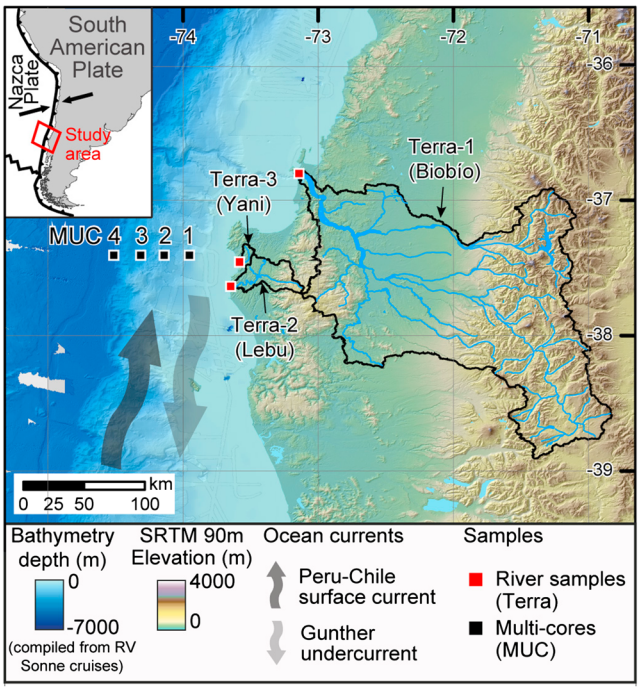

Figure 1. Overview of the study site. Three onshore river basins were sampled (Terra 1–3, black outline) that drain into the Pacific where, correspondingly, four multicorer (MUC 1–4) samples (black squares) of marine surface sediment were sampled.

2013], we obtained $[^{10}Be]_{reac}$. The concentrations of the reactive fraction of the major elements and $[^{9}Be]_{reac}$ were measured with inductively coupled plasma optical emission spectroscopy.

To compare terrigenous to marine sediment compositions and assess the terrigenous sediment loads from the Terra catchments to MUC sites, we carried out XRD (*X-ray diffraction*) on postleach silicate residuals of different apparent grain sizes and derived sediment loads for the terrestrial samples from in situ ^{10}Be-derived denudation rates.

4. Results

4.1. Mineralogical Sediment Composition and Terrestrial Sediment Loads

Given the different lithologies of Terra catchments [*Melnick and Echtler*, 2006] (Figure S1) and their difference in sediment export to the ocean (Table 1), the proportions at which the terrestrial samples mix before arriving at the MUC sampling points are unknown. We hence weighed the mineralogical composition and Be results (section 4.2) for their in situ ^{10}Be-derived sediment load (Table 1). The Biobío River has the largest sediment export to the shelf, outweighing the other two rivers in drainage area and sediment export; hence, this "load-weighed" mineralogical composition is mainly dominated by Biobío sediment. Some variations are present for plagioclase and kaolinite that most likely depend on the variable regional geology of each basin, but the overall similarity in mineralogical composition of the terrigenous and marine sediment generally supports previous provenance work [*Lamy et al.*, 1998; *Heberer et al.*, 2010].

Terrestrial denudation rates from in situ cosmogenic ^{10}Be used for load-weighing range from 65 t/km^2/yr for the Lebu to 429 t/km^2/yr for the Yani River basin (Tables 1 and S4). Such variations spanning 2 orders of magnitude in denudation could be caused by variable erodibility depending on lithology (see Figure S1) but agree broadly with elsewhere reported values for this region [*Carretier et al.*, 2014].

4.2. Elemental and Isotopic Results

4.2.1. Concentration Results

Differences in $[^{9}Be]_{reac}$, $[^{10}Be]_{reac}$, and major reactive elemental concentrations between replicate samples amount to less than 10% (Tables 2 and S1) and are within the reported analytical repeatability for optical emission spectroscopy and accelerator mass spectrometry measurements [*Wittmann et al.*, 2015]. The two apparent grain size fractions of MUC-1 and MUC-3 yield differences in some elemental concentrations of up to 40% (Table S3), which is most likely caused by the presence of varying proportions of smaller aggregated particles that may have slightly different mineralogical composition. Concentrations of most major reactive elements increase from the terrestrial to the marine realm (from highest to lowest relative increase: $[Ti]_{reac} > [Al]_{reac} > [Fe]_{reac} > [K]_{reac}$; Table S3).

We also calculated "load-weighed" $[^{9}Be]_{reac}$ and $[^{10}Be]_{reac}$ concentrations for the three "Terra" basins (Figure 2 and Table 2) that are closest to the values for the large Biobío River (Table 2).

A twentyfold increase in $[^{10}Be]_{reac}$ is observed from the terrestrial (load-weighed 0.44×10^8 at/g) to the marine realm (mean 9.5×10^8 at/g). For $[^{9}Be]_{reac}$, a 1.5-fold increase from a load-weighed concentration of

Table 2. ^{9}Be and ^{10}Be Concentrations and $^{10}Be/^{9}Be$ Ratios for Reactive (Sequentially Extracted) Phases[a]

Sample ID	Grain Size Analyzed[b] (μm)	Comments[c]	$[^{9}Be]$[d] (10^{16} at/g_{solid})	$[^{10}Be]$[e] (10^{8} at/g_{solid})	$^{10}Be/^{9}Be$[f] (10^{-8} at/g / at/g)
Terra-1 (Biobío)	<63	Replicate 1	1.563 ± 0.078	0.448 ± 0.015	0.287 ± 0.017
	<63	Replicate 2	1.630 ± 0.081	0.411 ± 0.014	0.252 ± 0.015
Terra-2 (Lebu)	<63		4.092 ± 0.205	1.451 ± 0.052	0.355 ± 0.022
Terra-3 (Yani)	<63		2.790 ± 0.139	1.080 ± 0.042	0.387 ± 0.025
Terra: Weighed for sediment load measured by in situ ^{10}Be[g]			1.745 ± 0.085	0.440 ± 0.016	0.252 ± 0.015
MUC-1	<63		2.155 ± 0.057	7.90 ± 0.26	3.60 ± 0.21
	125–250		2.86 ± 0.15	11.10 ± 0.33	3.74 ± 0.22
	<63[h]		2.36 ± 0.12	7.08 ± 0.22	3.00 ± 0.18
MUC-2	250–500[i]		2.66 ± 0.13	11.38 ± 0.57	4.27 ± 0.30
MUC-3	125–250	Replicate 1	2.80 ± 0.14	11.58 ± 0.58	4.14 ± 0.29
	125–250	Replicate 2	2.89 ± 0.14	12.13 ± 0.61	4.20 ± 0.30
	<63[h]		2.49 ± 0.12	9.15 ± 0.29	3.68 ± 0.22
MUC-4	125–250	Replicate 1	2.72 ± 0.14	7.93 ± 0.40	2.92 ± 0.21
	125–250	Replicate 2	2.52 ± 0.13	7.45 ± 0.37	2.96 ± 0.21
MUC: Average values ± 1 SD			2.60 ± 0.25	9.52 ± 2.02	3.61 ± 0.54

[a]Note that we provide separate results for the two performed leaching steps in the supporting information; "reac" phases provide the sum of the "am-ox" (1 M HCl-leached amorphous oxides) and the "x-ox" (hydroxylamine-leached crystalline oxides) steps. Prior to analysis negligible presence of biogenic components and carbonates was validated (see supporting information) as these components may change sedimentary meteoric ^{10}Be concentrations [*Southon et al.*, 1987; *Lal et al.*, 2006].
[b]Apparent grain sizes due to secondary particle formation revealed by laser granulometry data (supporting information).
[c]Replicate analysis (for ^{9}Be and ^{10}Be) performed on newly weighed sample splits. For most terrestrial samples, am-ox and x-ox steps of sequential extraction (see supporting information) were separately analyzed for ^{9}Be (but not for ^{10}Be). These separate results are given in supporting information Table S1. Given here are summed reactive (am-ox + x-ox) results.
[d]All ^{9}Be analyses except Terra-1 and MUC-2 are averages from two replicate leaches performed on newly weighed sample splits. Uncertainty is 1 SD of two replicates or 5% analytical uncertainty for Terra-1 and MUC-2.
[e]Uncertainty contains analytical uncertainty from AMS measurement, and sample ratio was corrected using a mean long-term blank $^{10}Be/^{9}Be$ ratio of 2.2(±2.5, 1 SD) × 10^{-15} (n = 28).
[f]Uncertainty contains a 5% uncertainty of single ^{9}Be measurements and the given ^{10}Be uncertainty.
[g]Load-weighed values (for terrestrial samples) calculated by weighing each value with the respective sediment load calculated from in situ ^{10}Be-derived denudaton rates (Table 1) (for in situ ^{10}Be methods description, see supporting information).
[h]Processed in 2015 by different operator.
[i]Coarser grain size analyzed due to negligible recovery for finer grain sizes (XRD performed on different grain size).

1.75 × 10^{16} at/g to a mean concentration of 2.60 × 10^{16} at/g (Figure 2 and Table 2) is observed that is marginally larger than observed grain size variations. Both increases in $[^{10}Be]_{reac}$ and $[^{9}Be]_{reac}$ take place between the coast and the MUC-1 sampling site. Between MUC-1 and MUC-4 (30 to 80 km from the coast), both isotopes are uniform.

4.2.2. Isotope and Elemental Ratio Results

When forming the ratio of ^{10}Be and ^{9}Be reactive concentrations $(^{10}Be/^{9}Be)_{reac}$, the differences observed for the different grain size fractions are mostly canceled out (Figure 2 and Table 2). The resulting $(^{10}Be/^{9}Be)_{reac}$ increase from rivers to ocean from a value of ~0.25 × 10^{-8} in Terra samples to ~3.6 × 10^{-8} in MUC samples (Figure 2c and Table 2). Importantly, the latter ratio is still lower than open Pacific Ocean values (see below). When we calculate the quotient of the net increases of $[^{10}Be]_{reac}$ (9.03 × 10^{8} at/g) and $[^{9}Be]_{reac}$ (0.83 × 10^{16} at/g), respectively (section 4.2.1), a $(^{10}Be/^{9}Be)_{reac}$ of 1.1 × 10^{-7} results. This ratio is similar to open Pacific Ocean $(^{10}Be/^{9}Be)_{reac}$ of marine surface sediment, surface-layer scrapes of Mn crusts, and dissolved $(^{10}Be/^{9}Be)_{diss}$ with a well-mixed open ocean value of ~1.2 × 10^{-7} (Figure 2c).

To assess whether Fe-Al oxyhdroxides are indeed the main carrier of Be, we normalized the concentrations of $[^{9}Be]_{reac}$ to $[Fe]_{reac}$, resulting in $(^{9}Be/Fe)_{reac}$. This normalization is reasonable as reactive Fe is affected similarly during the sequential extraction as Be [*Helz and Valette-Silver*, 1992], and Fe supplies the largest mass fraction of the sequentially extracted phases (Table S3). We find that $(^{9}Be/Fe)_{reac}$ does not significantly vary between different grain sizes, nor do they change from weighed river data to ocean (Figure 2d and Table S2).

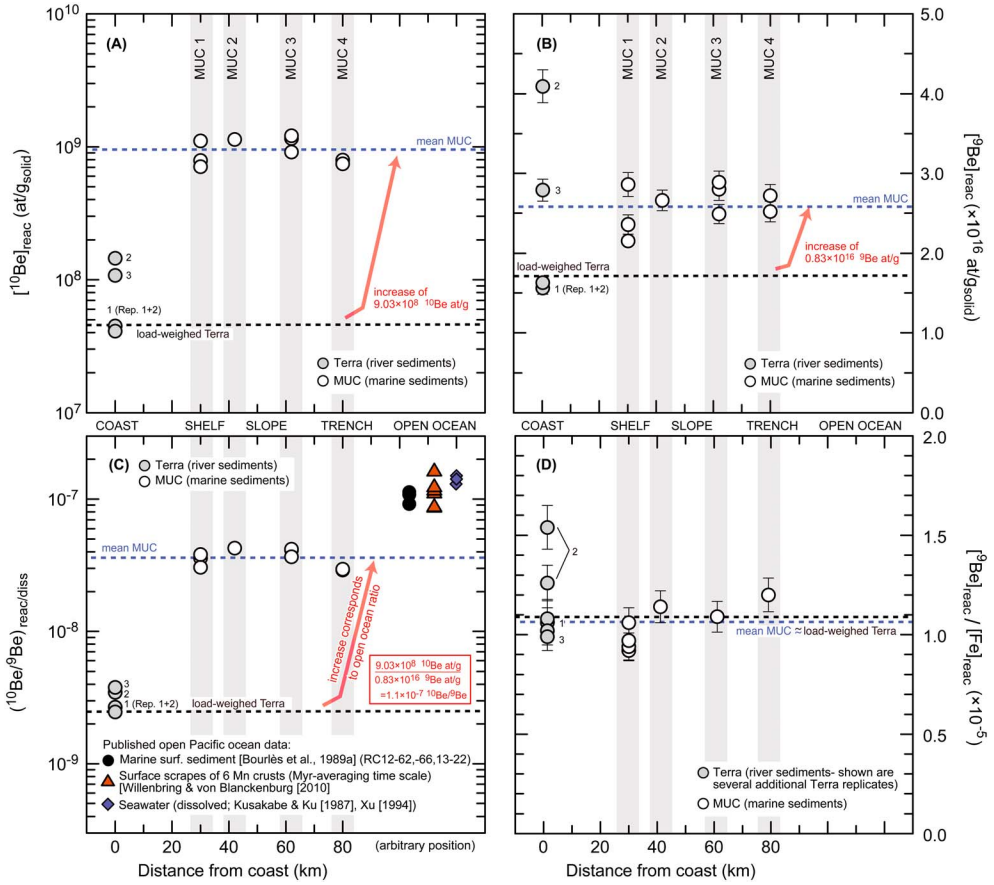

Figure 2. (a) $[^{10}Be]_{reac}$, (b) $[^{9}Be]_{reac}$, and (c) $(^{10}Be/^{9}Be)_{reac\ or\ diss}$ and (d) $^{9}Be/(Fe)_{reac} \times 10^{-5}$ from terrestrial samples (Terra 1–3) and marine surface sediments (MUC) versus increasing distance from the coast. Be data are given in Table 2, and Fe data are given in Table S3. If uncertainties are not shown they are smaller than symbol sizes; results from replicates or different grain size measurements superimpose each other in some cases. Black stippled lines give load-weighed terrestrial values (see text); blue stippled lines show mean of MUC data, and red arrows show increase from load-weighed terrestrial to mean MUC data (see text).

5. Discussion

5.1. Preservation of a Terrestrial Phase in Marine Surface Sediments

Our new data for $[^{10}Be]_{reac}$, $[^{9}Be]_{reac}$, and $(^{10}Be/^{9}Be)_{reac}$ show that in this near-coastal setting, measured $(^{10}Be/^{9}Be)_{reac}$ of authigenic phases contained in marine surface sediments have not reached open ocean values relative to their terrestrial source. That marginal sites show lower $^{10}Be/^{9}Be$ than their adjacent open ocean counterparts has been observed in the Baffin Bay [*Simon et al.*, 2016b] and at sites surrounding Papua New Guinea [*Ménabréaz et al.*, 2012, 2014], and from a Mediterranean marginal site [*Simon et al.*, 2017] (for summary of this published data, see Table S2).

Interestingly, we find that quotient of the net increases of $[^{10}Be]_{reac}$ to $[^{9}Be]_{reac}$ from rivers to ocean is in the same order as open ocean reactive and dissolved $^{10}Be/^{9}Be$. This means that the authigenic phases in marine surface sediment preserve a terrestrial phase and another, ocean-derived phase was later superimposed (Figure 3). The $(^{10}Be/^{9}Be)_{reac}$ of MUC samples (3.6×10^{-8}) hence is a mixture of the $(^{10}Be/^{9}Be)_{reac}$ of Terra samples (comprising ratios of 0.25×10^{-8}) and an open-ocean phase with the typical Pacific open ocean ratio ($\sim 1.1 \times 10^{-7}$).

These observations provide evidence that the authigenic phases in our MUC samples have formed under influence of deep ocean seawater at a distance of only 30 km from the coast (given that all MUC sites have the same $(^{10}Be/^{9}Be)_{reac}$ and relative increases in Be concentrations, respectively). The source is likely Pacific

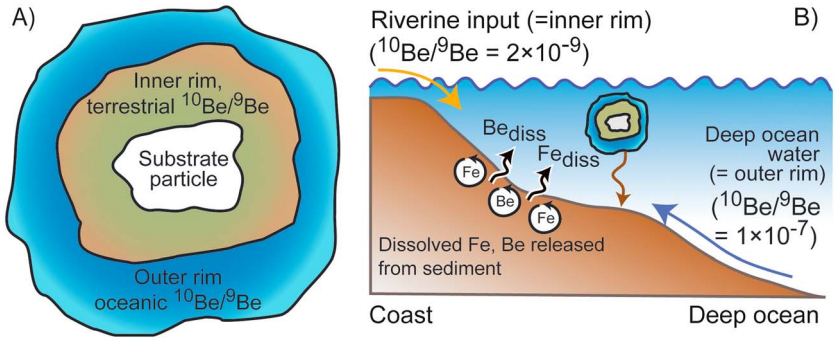

Figure 3. (a) Two-layer rim formation, the inner one preserving the sedimentary authigenic $^{10}Be/^{9}Be$ characteristic of continental erosion and the outer one preserving marine authigenic $^{10}Be/^{9}Be$ ratios. Sequential extractions removes both layers, resulting in a mixed (measured) $^{10}Be/^{9}Be$ ratio. (b) Setting the $^{10}Be/^{9}Be$ ratio in coast-proximal sites affected by deep water masses. Boundary exchange releases dissolved Fe and ^{9}Be into the sediment that are, together with a deep open ocean-$(^{10}Be/^{9}Be)_{reac}$ ratio, incorporated into authigenic phases.

Deep Water (PDW) with deep Pacific $(^{10}Be/^{9}Be)_{diss}$ [*Kusakabe et al*., 1987; *Xu*, 1994]. Note that in case of a deep water source, scavenging does not change the $^{10}Be/^{9}Be$ prevailing in seawater as both ^{10}Be and ^{9}Be are scavenged to the same degree [*von Blanckenburg and Igel*, 1999]. Only if isotope ratios differ regionally and scavenging efficiencies differ too, the dissolved $^{10}Be/^{9}Be$ ratios will be changed [*von Blanckenburg and Bouchez*, 2014].

5.2. Evidence for Diagenetic Release of Metals and Their Incorporation Into Reactive Rims

One possibility for the increase in $[Be]_{reac}$ in marine sediment samples is further adsorption of both Be isotopes from seawater. Solid-water partition coefficients log K_d of ^{9}Be are similar in rivers and seawater at about 4.9 to 5.5 compiled from studies using solely natural samples (excluding pure minerals and experimental approaches, e.g., *Aldahan et al*. [1999]), natural pH ranges of 6–8 and were within Be solubility ranges [*Chase et al*., 2002; *Luo and Ku*, 2004; *Wittmann et al*., 2015]. Indeed, when calculating sample-specific K_d from the increase in $[^{9}Be]_{reac}$ and $[^{10}Be]_{reac}$ in MUC samples and deep Pacific dissolved ^{10}Be concentrations of 2000 at/g and ^{9}Be of 30 pM, respectively [*Kusakabe et al*., 1987], we obtain a log K_d of exactly 5.6 for both isotopes. However, we observe a simultaneous increase in reactive Fe in roughly the same proportion as ^{9}Be, resulting in uniform $(^{9}Be/Fe)_{reac}$ from the terrestrial source to MUC sites (Figure 2d). Due to their reactive nature, only a small fraction of ^{9}Be and Fe are available in the dissolved form in seawater [*Measures and Edmond*, 1982; *Brown et al*., 1992a; *Johnson et al*., 1997]. Further, the mass ratio of Fe/Be in seawater is $\sim1 \times 10^{2}$ (calculated using a mean oceanic dissolved Fe concentration of 0.5 pM [*Achterberg et al*., 2001]), whereas that found in MUC samples is $\sim1 \times 10^{5}$ (Table S3). We thus discount adsorption as a significant process. Rather, a likely source of the high required amounts of dissolved Fe to be incorporated into marine authigenic phases is its release from pore waters during early diagenesis [*Canfield*, 1989; *Elrod et al*., 2004; *Staubwasser et al*., 2006]. Reductive dissolution of Fe-oxyhydroxides would release the trace metals coprecipitated with them, among them Be.

This possibility of pore water Fe release together with Be with an open-ocean $^{10}Be/^{9}Be$ ratio suggests that the formation of authigenic phases occurs via coprecipitation as reactive rims. We rule out the possibility of reversible adsorption, because adsorption cannot explain the simultaneous increase in reactive Fe and ^{9}Be to yield uniform $(^{9}Be/Fe)_{reac}$ ratios. Given that diagenetic release is a large source of dissolved Fe [*VanCappellen and Wang*, 1996], uniform $(^{9}Be/Fe)_{reac}$ ratios from the terrestrial to the oceanic environment can only be facilitated if the phase incorporating Fe and ^{9}Be grows in mass (Table S3), which is enabled through the formation of reactive rims during coprecipitation.

To summarize, by chemically extracting authigenic phases from marine surface sediment, we integrated over the "inner layer" of a reaction rim formed under terrestrial conditions, and the "outer layer" of the reaction rim that has formed on top of the inner layer in the marine realm. This outer layer must have formed near the

ocean floor where high dissolved Fe and ^{9}Be concentrations from pore water expulsion prevail, and under the influence of a deep water source, with a characteristic deep ocean ^{10}Be/^{9}Be (Figure 3).

6. Implications

Our most important finding is that cosmogenic ^{10}Be/^{9}Be ratios in the authigenic phase of marine sediment from near-coastal areas preserve isotope ratios set during continental erosion and riverine transport but onto these are superimposed ocean ratios set under marine conditions. We provide evidence that these phases are formed through coprecipitation, and not via reversible adsorption. Sequential leaching methods do not differentiate between these two phases and thus cannot resolve terrestrial versus oceanic sources. Besides the dissolved flux, desorption from terrigenous particles was speculated to present one of two net sources of ^{9}Be to seawater [*von Blanckenburg and Bouchez*, 2014; *von Blanckenburg et al*., 2015]. However, the increase in concentration in both Be isotopes in the sediment suggests that at this active continental margin setting the "boundary exchange" mechanism is one in which there is net loss of this reactive metal to the sediment, in line with the original "boundary scavenging" concept [*Anderson et al*., 1990].

Our study further has implications for the paleoflux information that authigenic ^{10}Be/^{9}Be records at a given ocean site will yield, provided that changing boundary conditions like sea level or oceanic circulation variations can be accounted for. In coast-proximal sites that are affected neither by deeper water nor by narrow boundary currents, the authigenic record may be dominated by the terrigenous source and thus preserves the riverine ratios unaffected by exchange with seawater. The authigenic phase of sediment will thus be a direct recorder of terrigenous denudation of the adjacent river catchments.

Open ocean sites, in contrast, are located on the ocean side of boundary currents where homogenization has occurred [*Igel and von Blanckenburg*, 1999; *von Blanckenburg and Igel*, 1999]. There, ^{10}Be/^{9}Be ratios will record ocean-basin wide weathering and denudation fluxes [*Willenbring and von Blanckenburg*, 2010b; *von Blanckenburg et al*., 2015] and global changes in cosmic ray production as modulated by magnetic field strength [*Christl et al*., 2003; *Carcaillet et al*., 2004; *Knudsen et al*., 2008; *Simon et al*., 2016a].

The continental margin site studied here is an intermediate one as it is positioned in the transition zone between terrigenous and open ocean-dominated fluxes. That this transition is located at only 30 km from the coast is attributed to the narrow eastern Pacific boundary current and influence of PDW seawater. A similar documented transitional site is the Baffin Bay at which ^{10}Be/^{9}Be shifts in a time-dependent manner between open ocean ratios and meltwater discharge [*Simon et al*., 2016b]. These marginal sites are probably best suited to decipher the hitherto elusive boundary exchange and the processes that contribute to it today, and back though time.

Acknowledgments
Additional information for this article can be found in the supporting information. This work was funded by German Science Foundation (DFG) grant WI 3874/2-1 and BE 5070/2-1 (to H. Wittmann and A. Bernhardt). The authors claim no conflicts of interest. We thank D. Melnick, J. Jara-Muñoz, and A. Tassara for acquisition of Terra samples, M. Oelze for help during laboratory work, C. Günter and D. Kauschuss for XRD support, and C. Andermann and S. Liening for performing grain size analysis in GFZ's "SedLab." We sincerely thank C. Jeandel and Q. Simon for constructive reviews that improved this manuscript.

References

Achterberg, E. P., T. W. Holland, A. R. Bowie, R. F. C. Mantoura, and P. J. Worsfold (2001), Determination of iron in seawater, *Anal. Chim. Acta*, *442*(1), 1–14.

Aldahan, A., H. P. Ye, and G. Possnert (1999), Distribution of beryllium between solution and minerals (biotite and albite) under atmospheric conditions and variable pH, *Chem. Geol.*, *156*(1–4), 209–229.

Anderson, R. F., Y. Lao, W. S. Broecker, S. E. Trumbore, H. J. Hofmann, and W. Wolfli (1990), Boundary scavenging in the Pacific Ocean: A comparison of ^{10}Be and ^{231}Pa, *Earth Planet. Sci. Lett.*, *96*(3–4), 287–304.

Anderson, R. F., E. Mawji, G. A. Cutter, C. I. Measures, and C. Jeandel (2014), GEOTRACES: Changing the way we explore ocean chemistry, *Oceanography*, *27*(1), 50–61.

Arsouze, T., J. C. Dutay, F. Lacan, and C. Jeandel (2009), Reconstructing the Nd oceanic cycle using a coupled dynamical—Biogeochemical model, *Biogeosciences*, *6*(12), 2829–2846.

Bernhardt, A., D. Hebbeln, M. Regenberg, A. Lückge, and M. R. Strecker (2016), Shelfal sediment transport by an undercurrent forces turbidity-current activity during high sea level along the Chile continental margin, *Geology*, *44*(4), 295–298.

Blott, S. J., and K. Pye (2001), GRADISTAT: A grain size distribution and statistics package for the analysis of unconsolidated sediments, *Earth Surf. Processes Landforms*, *26*(11), 1237–1248.

Borchers, B., S. Marrero, G. Balco, M. Caffee, B. Goehring, N. Lifton, K. Nishiizumi, F. Phillips, J. Schaefer, and J. Stone (2016), Geological calibration of spallation production rates in the CRONUS-Earth project, *Quat. Geochronol.*, *31*, 188–198.

Bourlès, D., G. M. Raisbeck, and F. Yiou (1989a), ^{10}Be and ^{9}Be in marine sediments and their potential for dating, *Geochim. Cosmochim. Acta*, *53*(2), 443–452.

Bourlès, D. L., G. Klinkhammer, A. C. Campbell, C. I. Measures, E. T. Brown, and J. M. Edmond (1989b), Beryllium in marine pore waters: Geochemical and geochronological implications, *Nature*, *341*(6244), 731–733.

Braucher, R., S. Merchel, J. Borgomano, and D. L. Bourlès (2011), Production of cosmogenic radionuclides at great depth: A multi element approach, *Earth Planet. Sci. Lett.*, *309*(1–2), 1–9.

Brown, E. T., C. I. Measures, J. M. Edmond, D. L. Bourles, G. M. Raisbeck, and F. Yiou (1992a), Continental inputs of beryllium to the oceans, *Earth Planet. Sci. Lett.*, *114*(1), 101–111.
Brown, E. T., J. M. Edmond, G. M. Raisbeck, D. Bourlès, F. Yiou, and C. I. Measures (1992b), Beryllium isotope geochemistry in tropical river basins, *Geochim. Cosmochim. Acta*, *56*, 1607–1624.
Canfield, D. E. (1989), Reactive iron in marine sediments, *Geochim. Cosmochim. Acta*, *53*(3), 619–632.
Carcaillet, J., D. L. Bourlès, N. Thouveny, and M. Arnold (2004), A high resolution authigenic $^{10}Be/^{9}Be$ record of geomagnetic moment variations over the last 300 ka from sedimentary cores of the Portuguese margin, *Earth Planet. Sci. Lett.*, *219*(3–4), 397–412.
Carretier, S., et al. (2014), Erosion in the Chilean Andes between 27°S and 39°S: Tectonic, climatic and geomorphic control, *Geol. Soc., London, Spec. Publ.*, *399*.
Chase, Z., R. F. Anderson, M. Q. Fleisher, and P. W. Kubik (2002), The influence of particle composition and particle flux on scavenging of Th, Pa and Be in the ocean, *Earth Planet. Sci. Lett.*, *204*(1–2), 215–229.
Christl, M., C. Strobl, and A. Mangini (2003), Beryllium-10 in deep-sea sediments: A tracer for the Earth's magnetic field intensity during the last 200,000 years, *Quat. Sci. Rev.*, *22*(5–7), 725–739.
Christl, M., C. Vockenhuber, P. W. Kubik, L. Wacker, J. Lachner, V. Alfimov, and H. A. Synal (2013), The ETH Zurich AMS facilities: Performance parameters and reference materials, *Nucl. Instrum. Methods Phys. Res., Sect. B*, *294*, 29–38.
Dunai, T. J. (2000), Scaling factors for production rates of in situ produced cosmogenic nuclides: A critical reevaluation, *Earth Planet. Sci. Lett.*, *176*(1), 157–169.
Elrod, V. A., W. M. Berelson, K. H. Coale, and K. S. Johnson (2004), The flux of iron from continental shelf sediments: A missing source for global budgets, *Geophys. Res. Lett.*, *31*, L12307, doi:10.1029/2004GL020216.
Frank, M., D. Porcelli, P. Andersson, M. Baskaran, G. Bjork, P. W. Kubik, B. Hattendorf, and D. Guenther (2009), The dissolved beryllium isotope composition of the Arctic Ocean, *Geochim. Cosmochim. Acta*, *73*(20), 6114–6133.
Hebbeln, D., and Cruise Participants (2001), *PUCK: Report and Preliminary Results of R/V Sonne Cruise SO 156, Valparaiso (Chile)—Talcahuano (Chile)*, 195 pp., Universität Bremen, Berichte aus dem Fachbereich Geowissenschaften der Universität Bremen, 29 March–14 May.
Heberer, B., G. Röser, J. H. Behrmann, M. Rahn, and A. Kopf (2010), Holocene sediments from the southern Chile trench: A record of active margin magmatism, tectonics and palaeoseismicity, *J. Geol. Soc.*, *167*(3), 539–553.
Helz, G. R., and N. Valette-Silver (1992), Beryllium-10 in Chesapeake Bay sediments: An indicator of sediment provenance, *Estuarine Coastal Shelf Sci. 34*(5), 459–469.
Igel, H., and F. von Blanckenburg (1999), Lateral mixing and advection of reactive isotopetracers in ocean basins: Numerical modeling, *Geochem. Geophys. Geosyst.*, *1*(1), 1002, doi:10.1029/1999GC000003.
Jeandel, C. (2016), Overview of the mechanisms that could explain the "Boundary Exchange" at the land–ocean contact, *Philos. Trans. R. Soc. London, Ser. A*, *374*(2081).
Jeandel, C., and E. H. Oelkers (2015), The influence of terrigenous particulate material dissolution on ocean chemistry and global element cycles, *Chem. Geol.*, *395*, 50–66.
Johnson, K. S., R. M. Gordon, and K. H. Coale (1997), What controls dissolved iron concentrations in the world ocean?, *Mar. Chem.*, *57*(3–4), 137–161.
Knudsen, M. F., G. M. Henderson, M. Frank, C. M. Niocaill, and P. W. Kubik (2008), In-phase anomalies in beryllium-10 production and palaeomagnetic field behaviour during the Iceland Basin geomagnetic excursion, *Earth Planet. Sci. Lett.*, *265*(3–4), 588–599.
Kusakabe, M., and T.-L. Ku (1984), Incorporation of be isotopes and other trace metals into marine ferromanganese deposits, *Geochim. Cosmochim. Acta*, *48*(11), 2187–2193.
Kusakabe, M., T. L. Ku, J. R. Southon, J. S. Vogel, D. E. Nelson, C. I. Measures, and Y. Nozaki (1987), Distribution of ^{10}Be and ^{9}Be in the Pacific Ocean, *Earth Planet. Sci. Lett.*, *82*(3–4), 231–240.
Kusakabe, M., T. Ku, J. Southon, and C. Measures (1990), Beryllium isotopes in the ocean, *Geochem. J.*, *24*(4), 263–272.
Kusakabe, M., T. L. Ku, J. R. Southon, L. Shao, J. S. Vogel, D. E. Nelson, S. Nakaya, and G. L. Cusimano (1991), Be isotopes in rivers/estuaries and their oceanic budgets, *Earth Planet. Sci. Lett.*, *102*(3–4), 265–276.
Lacan, F., and C. Jeandel (2005), Neodymium isotopes as a new tool for quantifying exchange fluxes at the continent–ocean interface, *Earth Planet. Sci. Lett.*, *232*(3–4), 245–257.
Lal, D., C. Charles, L. Vacher, J. N. Goswami, A. J. T. Jull, L. McHargue, and R. C. Finkel (2006), Paleo-ocean chemistry records in marine opal: Implications for fluxes of trace elements, cosmogenic nuclides (^{10}Be and ^{26}Al), and biological productivity, *Geochim. Cosmochim. Acta*, *70*(13), 3275–3289.
Lamy, F., D. Hebbeln, and G. Wefer (1998), Terrigenous sediment supply along the Chilean continental margin: Modern regional patterns of texture and composition, *Geol. Rundsch.*, *87*(3), 477–494.
Lao, Y., R. F. Anderson, W. S. Broecker, S. E. Trumbore, H. J. Hofmann, and W. Wolfli (1992), Transport and burial rates of ^{10}Be and ^{231}Pa in the Pacific Ocean during the Holocene period, *Earth Planet. Sci. Lett.*, *113*(1–2), 173–189.
Luo, S., and T.-L. Ku (2004), On the importance of opal, carbonate, and lithogenic clays in scavenging and fractionating ^{230}Th, ^{231}Pa and ^{10}Be in the ocean, *Earth Planet. Sci. Lett.*, *220*(1–2), 201–211.
Measures, C. I., and J. M. Edmond (1982), Beryllium in the water column of the central North Pacific, *Nature*, *297*(5861), 51–53.
Melnick, D., and H. Echtler (2006), Morphotectonic and geologic digital map compilations of the south-central Andes (36–42° S), in *The Andes*, edited, pp. 565–568, Springer.
Ménabréaz, L., D. L. Bourlès, and N. Thouveny (2012), Amplitude and timing of the Laschamp geomagnetic dipole low from the global atmospheric ^{10}Be overproduction: Contribution of authigenic $^{10}Be/^{9}Be$ ratios in west equatorial Pacific sediments, *J. Geophys. Res.*, *117*, doi:10.1029/2012JB009256.
Ménabréaz, L., N. Thouveny, D. L. Bourlès, and L. Vidal (2014), The geomagnetic dipole moment variation between 250 and 800 ka BP reconstructed from the authigenic $^{10}Be/^{9}Be$ signature in West Equatorial Pacific sediments, *Earth Planet. Sci. Lett.*, *385*(0), 190–205.
Muñoz, P., C. B. Lange, D. Gutiérrez, D. Hebbeln, M. A. Salamanca, L. Dezileau, J. L. Reyss, and L. K. Benninger (2004), Recent sedimentation and mass accumulation rates based on ^{210}Pb along the Peru–Chile continental margin, *Deep Sea Res. Part II*, *51*(20–21), 2523–2541.
Radic, A., F. Lacan, and J. W. Murray (2011), Iron isotopes in the seawater of the equatorial Pacific Ocean: New constraints for the oceanic iron cycle, *Earth Planet. Sci. Lett.*, *306*(1), 1–10.
Segl, M., et al. (1984), ^{10}Be-dating of a manganese crust from central North Pacific and implications for ocean palaeocirculation, *Nature*, *309*(5968), 540–543.
Simon, Q., N. Thouveny, D. L. Bourlès, J.-P. Valet, F. Bassinot, L. Ménabréaz, V. Guillou, S. Choy, and L. Beaufort (2016a), Authigenic $^{10}Be/^{9}Be$ ratio signatures of the cosmogenic nuclide production linked to geomagnetic dipole moment variation since the Brunhes/Matuyama boundary, *J. Geophys. Res. Solid Earth*, *121*, 7716–7741.

Simon, Q., N. Thouveny, D. L. Bourlès, L. Nuttin, C. Hillaire-Marcel, and G. St-Onge (2016b), Authigenic $^{10}Be/^{9}Be$ ratios and ^{10}Be-fluxes ($^{230}Th_{xs}$-normalized) in central Baffin Bay sediments during the last glacial cycle: Paleoenvironmental implications, *Quat. Sci. Rev*, *140*, 142–162.

Simon, Q., et al. (2017), Authigenic $^{10}Be/^{9}Be$ ratio signature of the Matuyama–Brunhes boundary in the Montalbano Jonico marine succession, *Earth Planet. Sci. Lett.*, *460*, 255–267.

Southon, J. R., T. L. Ku, D. E. Nelson, J. L. Reyss, J. C. Duplessy, and J. S. Vogel (1987), ^{10}Be in a deep-sea core: Implications regarding ^{10}Be production changes over the past 420 ka, *Earth Planet. Sci. Lett.*, *85*(4), 356–364.

Staubwasser, M., F. von Blanckenburg, and R. Schoenberg (2006), Iron isotopes in the early marine diagenetic iron cycle, *Geology*, *34*(8), 629–632.

Strub, P. T., J. M. Mesias, V. Montecino, J. Ruttlant, and S. Salinas (1998), Coastal ocean circulation off western South America, coastal segment (6, E), in *The Global Coastal Ocean. Regional Studies and Syntheses*, edited by A. R. Robinson and K. H. Brink, pp. 273–315, Wiley, New York.

Tessier, A., P. G. C. Campbell, and M. Bisson (1979), Sequential extraction procedure for the speciation of particulate trace metals, *Anal. Chem.*, *51*(7), 844–851.

Tolorza-Tolorza, V. (2015), Magnitud y dinámica de la erosión integrada de cuenca en el río Biobío, PhD thesis, 165 pp., Universidade de Chile, Santiago de Chile.

VanCappellen, P., and Y. F. Wang (1996), Cycling of iron and manganese in surface sediments: A general theory for the coupled transport and reaction of carbon, oxygen, nitrogen, sulfur, iron, and manganese, *Am. J. Sci.*, *296*(3), 197–243.

von Blanckenburg, F., and J. Bouchez (2014), River fluxes to the sea from the ocean's $^{10}Be/^{9}Be$ ratio, *Earth Planet. Sci. Lett.*, *387*(0), 34–43.

von Blanckenburg, F., and H. Igel (1999), Lateral mixing and advection of reactive isotope tracers in ocean basins: Observations and mechanisms, *Earth Planet. Sci. Lett.*, *169*, 113–128, doi:10.1029/1999GC000003.

von Blanckenburg, F., R. K. O'Nions, N. S. Belshaw, A. Gibb, and J. R. Hein (1996), Global distribution of beryllium isotopes in deep ocean water as derived from Fe-Mn crusts, *Earth Planet. Sci. Lett.*, *141*, 213–226.

von Blanckenburg, F., J. Bouchez, D. E. Ibarra, and K. Maher (2015), Stable runoff and weathering fluxes into the oceans over quaternary climate cycles, *Nat. Geosci.*, *8*(7), 538–542.

Willenbring, J. K., and F. von Blanckenburg (2010a), Long-term stability of global erosion rates and weathering during late-Cenozoic cooling, *Nature*, *465*(7295), 211–214.

Willenbring, J. K., and F. von Blanckenburg (2010b), Meteoric cosmogenic beryllium-10 adsorbed to river sediment and soil: Applications for Earth-surface dynamics, *Earth Sci. Rev.*, *98*(1–2), 105–122.

Wilson, D. J., A. M. Piotrowski, A. Galy, and I. N. McCave (2012), A boundary exchange influence on deglacial neodymium isotope records from the deep western Indian Ocean, *Earth Planet. Sci. Lett.*, *341–344*, 35–47.

Wittmann, H., and F. von Blanckenburg (2016), The geological significance of cosmogenic nuclides in large lowland river basins, *Earth Sci. Rev.*, *159*, 118–141.

Wittmann, H., F. von Blanckenburg, J. Bouchez, N. Dannhaus, R. Naumann, M. Christl, and J. Gaillardet (2012), The dependence of meteoric ^{10}Be concentrations on particle size in Amazon River bed sediment and the extraction of reactive $^{10}Be/^{9}Be$ ratios, *Chem. Geol.*, *318–319*(0), 126–138.

Wittmann, H., F. von Blanckenburg, N. Dannhaus, J. Bouchez, J. L. Guyot, L. Maurice, H. Roig, N. Filizola, J. Gaillardet, and M. Christl (2015), A test of the new cosmogenic ^{10}Be(meteoric)/^{9}Be proxy for simultaneously determining basin-wide erosion rates, denudation rates, and the degree of weathering in the Amazon basin, *J. Geophys. Res. Earth Surf*, *120*, 2498–2528, doi:10.1002/2015JF003581.

Xu, X. (1994), Geochemical studies of beryllium isotopes in marine and continental natural systems, PhD thesis, 315 pp., Univ. of Southern Calif., Los Angeles.